Soft Hybrid Elastomers Containing Polymer Grafted Nanoparticles

Jensen N. Sevening,[a‡] Siyana Dottin,[a‡] Vincent M. Torres,[b] and Robert J. Hickey[a,c,*]

[a]Department of Materials Science and Engineering, The Pennsylvania State University, University Park, PA 16802, USA

[b]Department of Chemistry, The Pennsylvania State University, University Park, PA 16802, USA

[c]Materials Research Institute, The Pennsylvania State University, University Park, PA 16802, USA

[‡]Co-first authors contributed equally

*Corresponding author: rjh64@psu.edu

Abstract

Soft elastomers containing inorganic nanoparticles are of interest for uses in soft robotics and flexible electronics, and successful implementation into these applications require enhanced material toughness while maintaining low moduli and high recovery. Controlling nanoparticle dispersion in hybrid materials is necessary to tune physical properties, yet many synthetic methods used to create filled rubbers often lead to macrophase separation. Therefore, alternative synthetic methods are required. Here, we report the synthesis of hybrid elastomers containing polymer grafted nanoparticles (PGNPs) covalently bound to a rubbery matrix. Specifically, poly(norbornene) grafted silica nanoparticles are initially dispersed in a lauryl methacrylate monomer and crosslinker mixture, and then polymerized to create the hybrid elastomer. The polymerization process, termed reaction-induced phase transitions (RIPT), to simultaneously crosslink and trap the nanoparticles in the polymer matrix is a versatile method for preparing soft hybrid elastomers. With increasing nanoparticle loading (e.g., 0 to 10 wt%), PGNP aggregates begin to form and there is an increase in the modulus. Interestingly, there is minimal impact on

tensile strength and elastic recovery with respect to PGNP loading as compared to that of the neat, crosslinked matrix. As reported here, the RIPT process is easily adaptable to crosslinked rubbery matrices, highlighting the versatility of the process.

Graphical Abstract

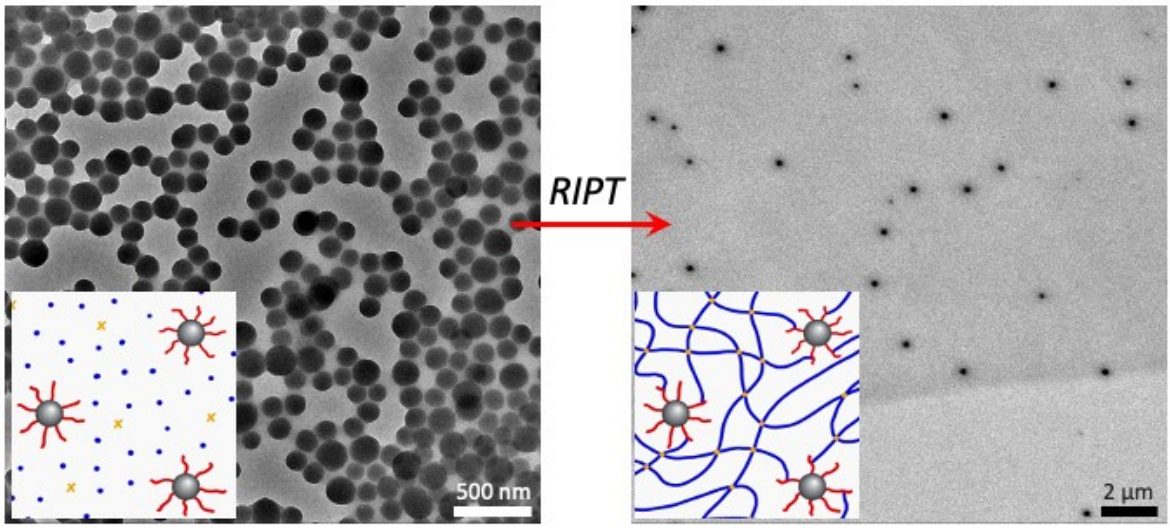

Keywords: Hybrid Elastomers, Polymer Grafted Nanoparticles, Nanocomposite, Polymerization, Reaction-Induced Phase Transitions, Mechanical Properties

1. Introduction

Hybrid polymeric materials seek to enhance neat polymer performance through the addition of fillers that are selected to access new properties unavailable to polymer-only systems[1-3] or further enhance properties inherent to polymer systems.[4-7] To access improved material properties, nanoparticle dispersion control is stringently important. To overcome nanoparticle dispersion challenges, polymer grafted nanoparticles (PGNPs) have shown promise in that a variety of dispersion states including well-dispersed, sheets, strings, and clusters are possible by tuning the polymer molecular weight grafted on the polymer and the matrix.[8,9] Multi-component hybrid systems composed of a polymer matrix containing inorganic nanoparticle filler, tend to have a thermodynamic drive towards phase separation.[10] The drive to phase separate is partially due to the immiscible organic-inorganic interactions. Thus, by grafting the nanoparticle surface with the same polymer as the matrix, the enthalpic "penalty" to mixing is neutralized, improving filler dispersion.[8,11] There is extensive literature pertaining to PGNP filled polymer matrices,[8,11] however, these studies tend to focus on glassy thermoplastics such as poly(styrene) and poly(methyl methacrylate).[12] Thus, to fully realize and harness the benefits of adding PGNPs to polymer materials, alternative methods are needed to expand the scope of materials to broaden application uses.

Soft elastomers (e.g., material modulus on the order of 100s of kPa)[13,14] are a subset of elastomers that have potential uses in soft robotics,[15] dielectric actuators,[16-18] magnetoactive elastomers,[19-21] biomedical applications,[22,23] and flexible electronics.[24] Successful material design requires a balance between low modulus, high toughness, and recoverable elasticity under high strain to ensure long performance lifetimes. When utilizing hybrid materials, filler dispersion and

resulting component interfacial contacts are known to have a significant role in mechanical properties.[25] Current filled rubbers, most notably rubber tires, tend to result in microscale clustered filler dispersions that increase toughness, but at significantly higher moduli (e.g., on the order of 10s of MPa).[26,27] For soft hybrid elastomers, an increase in toughness without significant increase to modulus requires low polymer matrix crosslinking with controlled nanoparticle dispersion. Therefore, incorporating PGNPs within soft, crosslinked matrices to dictate filler dispersion and thus physical properties is necessary to advance the nanocomposite field.[8]

Previous work has shown the ability to control nanoparticle dispersion within an immiscible polymer matrix via a reaction-induced phase transition (RIPT).[28,29] Specifically, well-dispersed poly(cyclooctadiene) (PCOD) grafted nanoparticles in either a poly(styrene) (PS) or poly(methyl methacrylate) (PMMA) matrix was possible through a kinetic trapping and functionalization process during the polymerization of the PGNP/monomer mixture.[29] Nanoparticle dispersion within the final solid material was maintained throughout the bulk polymerization of the initial liquid monomer/PGNP mixture at high conversions. The unsaturated grafted PCOD chains promoted polymer functionalization due to the formation of allylic radicals during the bulk polymerization.[29] Allylic radicals on the PCOD chains form due to hydrogen abstraction via a radical initiator (e.g., benzoyl peroxide) and will initiate the polymerization of either styrene of methyl methacrylate.[29] Thus, PCOD is functionalized with polymer of the same chemical composition of the polymer matrix, enhancing PGNP dispersion. The in situ process of polymer functionalization via allylic radicals is akin to the synthesis of high-impact poly(styrene) in which poly(styrene) chains functionalize poly(butadiene), stabilizing the rubbery domains in a glassy matric.[30] Allylic radical-assisted polymer functionalization has also been shown to drive

nanoscale transitions in poly(butadiene)-based AB and ABA diblock and triblock copolymers, respectively.[31-33] The grafting of the matrix polymer onto the PGNP further aids in neutralizing the enthalpic mixing barriers between the inorganic component and polymer matrix by improving the miscibility of the particle surface with the matrix.

Herein, we report a new class of PGNP filled soft elastomers using RIPT that exhibit controlled nanoparticle dispersion while maintaining low material modulus. The soft hybrid elastomers are synthesized by initially dispersing poly(norbornene) (PNBE)-grafted silica nanoparticles within a lauryl methacrylate/1,6 hexanediol dimethacrylate mixture and then running the polymerization to form a crosslinked poly(lauryl methacrylate) (PLMA) matrix containing PGNPs. The mechanism of allylic radical formation promoting PLMA functionalization of the PNBE chains is predicted to improve component mixing, while simultaneously acting as a crosslinking component. The hybrid elastomers containing 5 wt% PGNP loading maintain low modulus (e.g., < 200 kPa) and elastic recoverability when stretched to 50% strain. The RIPT process reported is versatile and will open new avenues for synthesizing hybrid elastomers with different PGNPs to tailor material properties.

2. Results and Discussion

2.1 Synthesis of Hybrid Elastomers

Soft hybrid elastomers were synthesized by polymerizing a lauryl methacrylate/1,6 hexanediol dimethacrylate mixture containing PNBE-grafted silica nanoparticles, resulting in a crosslinked poly(lauryl methacrylate) (PLMA) matrix filled with PGNPs (**Figure 1**). PLMA was chosen as the matrix due to the low glass transition temperature (T_g = -55 °C, **Figure S2**) and the

similar methacrylate chemistry used in LaNasa *et al*,[29] which has been shown to lead to polymer grafting from polymer chains grafted to the nanoparticle surface. The PLMA matrix is polymerized in the presence of 1,6 hexanediol dimethacrylate crosslinker to achieve a lightly crosslinked elastomer network. The neat elastomer was initially synthesized with varying degrees of crosslinker (0.25-1.5 mol%) for 6 h at 80 °C via a bulk free radical polymerization initiated by benzoyl peroxide (BPO) (21.4 mg/mL LMA) in square Teflon molds. Once polymerized, films were swelled in isopropanol overnight to remove the sol fraction (e.g., unreacted monomer, crosslinker, and uncrosslinked oligomers) and then dried under vacuum. Dog bones were then punched out of the soft films for uniaxial extension tensile measurements. The measured elastic modulus of neat elastomers ranged from 88 to 459 kPa, increasing with increased crosslink density (**Figures S3** and **S4**). Crosslinker content less than 0.25 mol% resulted in incomplete networks, thus 0.25 mol% was the lowest crosslinking amount used to obtain a uniform network with the lowest measured modulus. The crosslinking conditions were then used in the synthesis of PGNP filled hybrid elastomers.

PGNPs were prepared through the grafting of polynorbornene (PNBE) from silica nanoparticle surfaces via surface-initiated ring opening metathesis polymerization (SI-ROMP), which is modified from previously published methods.[34-36] Hybrid elastomers are prepared by dispersing the PGNPs in a LMA, BPO, and crosslinker mixture and performing the polymerization, which results in a liquid-to-solid transition that is driven by the polymerization (e.g., reaction-induced phase transition (RIPT)). PGNPs were dispersed in the LMA monomer mixture through sonication and the elastomer thermosetting was performed through replication of the procedure described earlier for the unfilled crosslinked elastomers (**Figure 1a**). The materials

are predicted to contain two types of crosslink points: one is the “traditional” crosslink where a quaternary junction is formed when two PLMA chains are connected by a difunctional acrylate and the other is the PGNP where PLMA functionalizes the PNBE brush of the PGNP. PNBE chains functionalized with PLMA are predicted to form via allylic radicals on the PNBE chains, which provides an initiation point. The two covalent junctions (e.g., crosslinker and PGNP) are expected to increase the modulus of the material and aid in maintaining particle dispersion. PLMA functionalization of the PNBE chains on the particle is also hypothesized to improve particle dispersion by improving the miscibility of the PGNPs with the growing matrix, as the brush will appear more PLMA-like as grafting continues. Four hybrid elastomers were prepared by varying the nanoparticle weight fraction from 1-10 wt%. An optical transition from clear to opaque can be seen in the materials as the nanoparticle fraction increases due to the scattering of light caused by the increasing weight fraction of particles (**Figure 1b**).

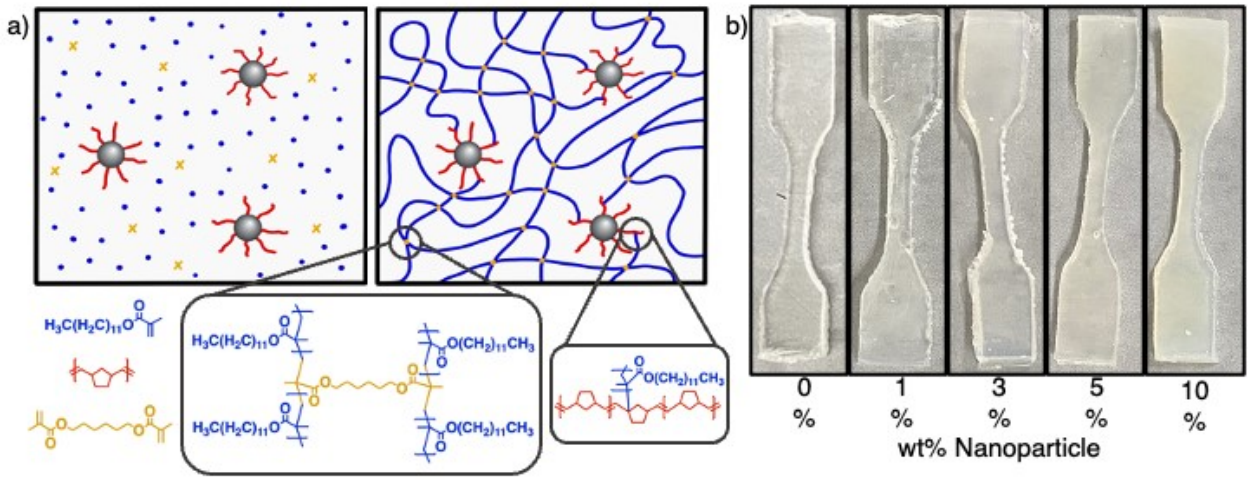

Figure 1. Scheme describing the synthesis of soft hybrid elastomers. a) Reaction scheme showing the free radical polymerization of lauryl methacrylate (blue), 1,6 hexanediol dimethacrylate (yellow), and PNBE grafted silica nanoparticles (red and grey) to produce thermoset hybrid

elastomers with a PLMA matrix and a PGNP filler. The BPO initiator is not pictured. b) Photographs of hybrid elastomer materials cut into dog bones with increasing nanoparticle weight percent (e.g., 0, 1, 3, 5, and 10 wt%, left to right).

The polymer grafted nanoparticles used in the study were prepared by first synthesizing silica nanoparticles of diameter 153 nm via the Stöber method,[37] in which particle growth is observed by the transition of the reaction solution from clear to opaque. Then norbornyl triethoxysilane is added to the reaction mixture to functionalize the particle surface and to provide a grafting site from which to initiate SI-ROMP. After activating the functional nanoparticles with Grubbs 3rd generation catalyst (G3), SI-ROMP is performed using a method developed by LaNasa *et al*[34] in which the activated nanoparticles are added to a norbornene monomer solution (38 g, 4 M in tetrahydrofuran). The polymerization is terminated by adding excess ethyl vinyl ether, which coordinates with the G3 catalyst, rendering it inactive by removing it from the growing chain end.[38,39] The addition of 3-bromopyridine (0.02M) to the initial norbornene solution decreases catalyst activity, resulting in a decrease in the polymer dispersity (**Figure 2a**). The resulting PGNPs have graft density of 0.12 chains/nm^2, a number-average molecular weight of M_n = 115 kg/mol, and a dispersity of $Đ$ = 1.10 (**Figures 2b** and **S7**). The hydrodynamic diameter measured using dynamic light scattering (DLS) of the particles before and after SI-ROMP show an increase from 154 nm to 353 nm, which is indicative of a solvent swollen brush height of approximately 100 nm. The hydrodynamic diameter of the PGNP was measured in lauryl methacrylate (3 mg/mL) (**Figure 2c**). The mixture is visibly clear, indicating a homogenous mixture in which the nanoparticles are soluble in the monomer. A homogeneous mixture is also supported by the monomodal distribution of particle size, which means there are no aggregates in the solution.

Furthermore, the transmission electron microscopy image in **Figure 2d** shows that there is a polymer layer around the nanoparticles.

The discrepancy in brush heights observed in TEM and measured in DLS is highly influenced by the sample environment. In DLS, the PGNPs are in good solvent conditions, and thus, the polymer chains are swollen and extend from the particle surface.[40] In TEM, PGNPs are prepared as a dry film, and brush heights are shortened due to theta conditions. Furthermore, polymer chain conformations are influenced by nearby particles and the surface of the TEM grid. Work by Ethier and Hall on modeling of PGNPs has shown increases in interpenetration of neighboring particles with decreasing graft density and increasing molecular weight.[41] Additionally, Ethier and Hall have shown these parameters and surface interaction of adsorbed polymers to produce "canopy" structures opposed to uniform spherical particles which influences the PGNP height.[42] With these considerations and the fact that that a "perfect" nanoparticle monolayer on the TEM grid was not achieved, the difference in polymer brush height between DLS and TEM are expected.

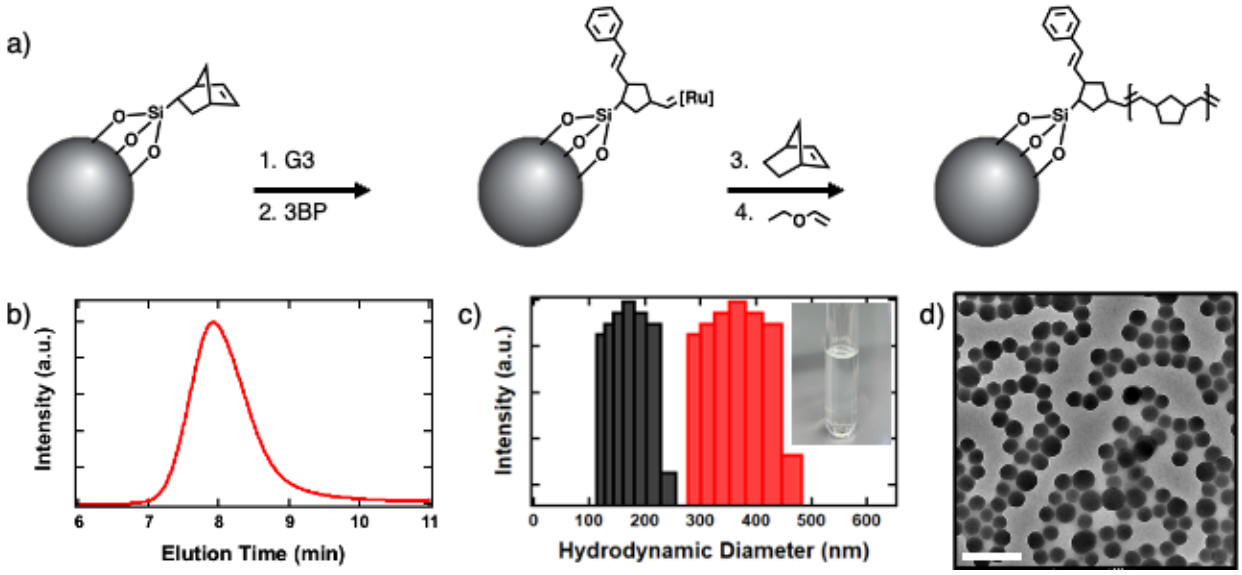

Figure 2. Characterization of the PGNP. a) Reaction scheme of SI-ROMP to produce PNBE grafted silica nanoparticles. b) Size-exclusion chromatography – multiangle light scattering detector (SEC-MALS) trace of the PNBE cleaved from the silica nanoparticle surface. c) DLS histograms showing the measured hydrodynamic diameter of NPs before (black) and after (red) SI-ROMP. DLS of the PGNPs was conducted using lauryl methacrylate as the solvent. Inset photograph shows the PGNPs in a lauryl methacrylate solution (3 mg/mL). d) TEM image of PNBE-grafted nanoparticles. Scale bar is 500 nm.

2.2 Microstructural Analysis

To tune desirable hybrid properties, interfacial interaction between the particles and the matrix plays a significant role, emphasizing the need for controlled filler dispersion.[25] It is predicted that functionalizing PNBE chains with PLMA will promote uniform dispersion of the particles in the hybrid elastomer in a two-fold manner. First, the functionalization of the PNBE chains with PLMA will reduce the enthalpic contribution to phase separate during the polymerization. Secondly, a thermoset matrix was anticipated to prevent nanoparticle aggregation

by hindering nanoparticle mobility by the presence of crosslinks. To test the two predictions, TEM images of the four different samples, prepared by microtoming the hybrid elastomers, were taken to assess particle distribution (**Figure 3**). As seen in **Figure 3**, small PGNP clusters form for all samples and the size of the clusters increases with increasing nanoparticle wt%. The nanoparticle center-to-center distance in the aggregates is on average constant, which is expected due to the grafted polymers on the surface of the PGNPs. Although the size of the nanoparticle clusters increases with increased nanoparticle weight fraction, the clusters are still isolated and do not form a percolated network even at the highest PGNP loading (e.g., 10 wt%), indicating the lack of macrophase separation. Interestingly, if the PGNP/PLMA system considered here is compared to the morphology diagram that is plotted as the product of the polymer grafting density and square root of the grafted polymer degree of polymerization ($\sigma\sqrt{N}$) versus the ratio of the polymer matrix and grafted polymer degrees of polymerization (P/N),[8] one would expect a phase separated mixture because $\sigma\sqrt{N} \approx 4$ for the PGNP and $P/N \rightarrow \infty$ due to the formation of a fully crosslinked PLMA matrix. Therefore, we predict that the initially homogeneous reactant mixture prior to the polymerization phase separates during the polymerization via a nucleation and growth mechanism, but the fully crosslinked matrix prevents macrophase separation.

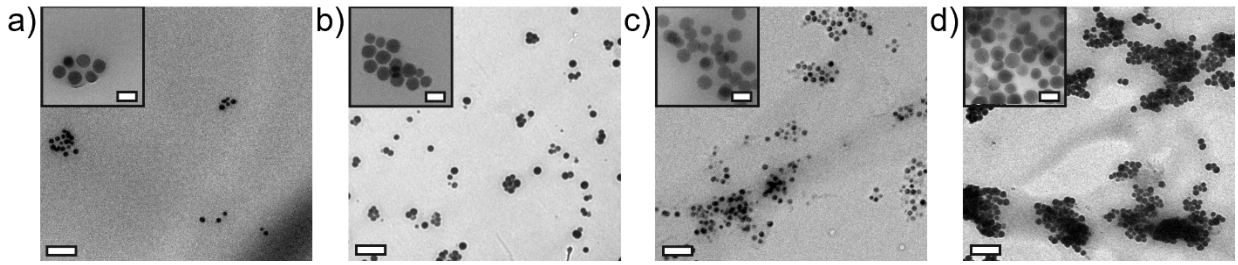

Figure 3. TEM micrographs of hybrid elastomers with a) 1, b) 3, c) 5, and d) 10 wt% nanoparticles.

PGNP clusters increase in size as the wt% increases. Samples were prepared by microtoming (Scale bar 1 μm). The inset images show PGNP aggregates at higher magnifications (Scale bar 200 nm).

2.3 Mechanical Analysis

The introduction of PGNPs into a polymer matrix is known to have a significant impact on the mechanical properties of a material.[25,43] To evaluate the mechanical performance of the synthesized hybrid elastomers, dog bones samples were cut from the bulk materials, and elastic modulus (*E*) and tensile strength (*TS*) were measured using uniaxial extension until sample break (**Figure 4**). For each sample with different nanoparticle loadings, 3 – 7 dog bone samples were prepared and measured to calculate the statistical mechanical property averages. The elastic modulus of the hybrid samples increases from 88 kPa for the neat sample to 121 and 158 kPa with 1 and 3 wt% NP respectively. The elastic modulus plateaus for 5 and 10 wt% samples, which were measured to be 153 and 164 kPa, respectively. However, the modulus trend is not consistent with tensile strength for the same samples. The average tensile strength at the sample break value for the neat and 1 wt% NP elastomer samples are within error (e.g., 74 kPa and 75 kPa, respectively). Tensile strength values slightly increase with the addition of 3 and 5 wt% NP, reaching the largest increase to 124 kPa for the 10 wt% NP sample. Thus, there seems to be a disconnect between material elastic modulus and tensile strength. In the case of elastic modulus, nanoparticles have a significant impact at low particle loadings, but levels off at higher loadings and vice versa for tensile strength. Thus, the results indicate that one potential benefit of the reported synthetic approach is that PGNPs will selectively enhance some properties of elastomers while preserving others.

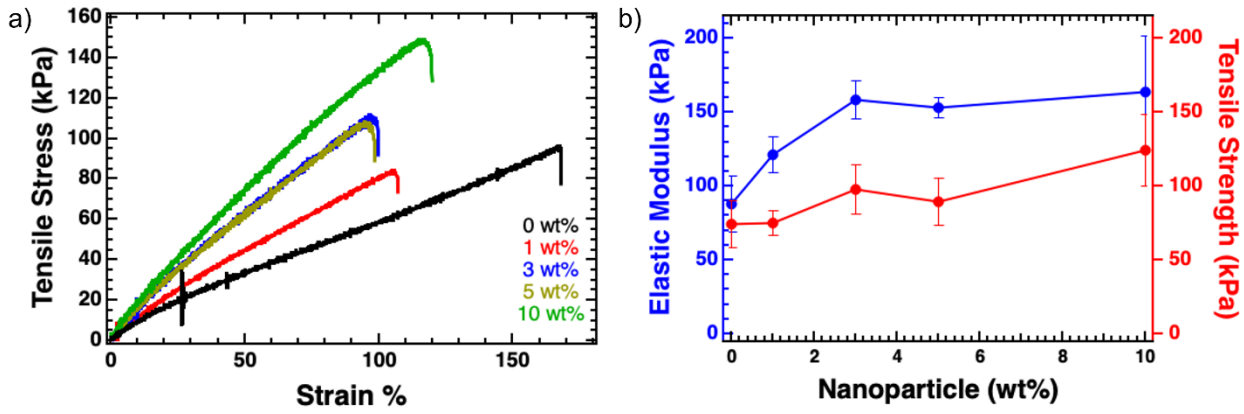

Figure 4. Mechanical property measurements for the synthesized hybrid elastomers. a) Representative uniaxial stress-strain curves of hybrid PLMA elastomers with the addition of 0 (black), 1 (red), 3 (blue), 5 (gold), or 10 (green) wt% PGNP loadings. Measurements were conducted at a 5 mm/min strain rate and 3 – 7 dog bone samples were prepared and measured for each sample composition. Only one representative stress-strain curve is shown for each sample. b) Summary of mechanical property results obtained from the stress-strain curves showing trends in elastic modulus (blue) and tensile strength (red) with increasing PGNP wt%.

Cyclic uniaxial extension measurements were conducted to assess the elastic recovery of the samples after deformation. Dog bone samples were measured in a similar fashion as the uniaxial extension measurements, however instead of straining to break, samples were extended and unloaded to their original position in repetitive cycles from 5 to 50% strain in increments of 5% for a total of 10 cycles. **Figure 5** shows the results of the recoverability tests at the even cycles, equivalent to strains of 10, 20, 30, 40, and 50% for both the neat and 5 wt% samples. Both stress-

strain plots show minimal hysteresis occurring, showing that recoverability is persevered, regardless of particle loading.

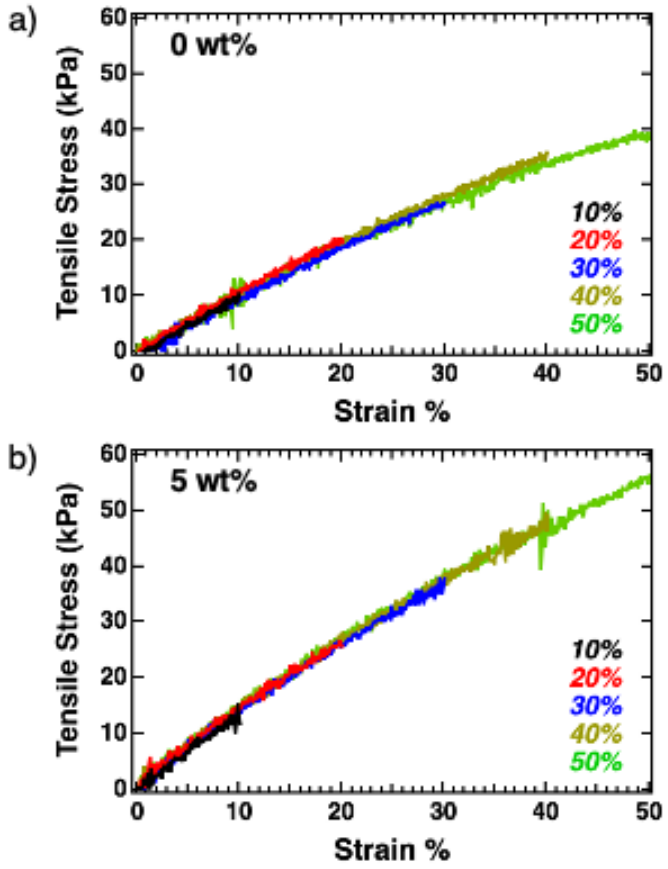

Figure 3. Cyclic uniaxial extension measurements showing material recoverability for the a) neat and b) 5 wt% hybrid PLMA elastomers with strains up to 10 (black), 20 (red), 30 (blue), 40 (gold), and 50 (green) %. Each sample was run in duplicate and representative traces are shown.

The previous reports utilizing RIPT to synthesize hybrid materials highlight how simultaneously polymerizing monomer and nanoparticles together lead to either trapping or controlling nanoparticle organization in a facile and an effective manner.[28,29] The work presented

here adapts the RIPT technique for the formulation of soft elastomeric hybrid materials where the influence of particle fillers is hypothesized to have a much greater impact on the range of mechanical performance. We predict that PGNP dispersion is controlled by the degree of: 1) PLMA functionalization on PNBE and 2) crosslinking, which would limit particle mobility (i.e., similarly/comparatively as a glassy matrix would). However, the PLMA/PGNP material system formed PNGP clusters that do not macrophase separate, which is different from the materials composed of either a PS or PMMA glassy matrix. With the PCOD grafted nanoparticles in either PS or PMMA, there were highly dispersed nanoparticles whereas with PNBE grafted nanoparticles in rubbery PLMA, the nanoparticles form a dispersion of aggregated clusters. The low level of crosslinking used in this study is likely not enough to compensate for the hindered mobility afforded by a glassy matrix.[44] It is predicted that there would be a greater enhancement in the mechanical properties (e.g., elastic modulus, tensile strength, and strain at break) of the soft elastic hybrid materials reported here if uniform nanoparticle dispersion is achieved, which is supported by previously published work from Kumar and coworkers.[45,46] Thus, further experimentation on dispersion impact from varied crosslink density is required. Additionally, it is worthwhile to address the difference in chemistries involved, as it is assumed that PLMA is grafting from the PGNP in the same fashion as the PS and PMMA. Both PNBE and PCOD are unsaturated polymers, thus both will form allylic radicals. However, free radical allylic initiated polymerizations randomly occur, and the number to junction points from the polymer grafted to the nanoparticle surface is difficult to quantify.

3. Conclusion

Expanding the functionality of soft hybrid elastomers with nanoparticle additives while maintaining the mechanical properties of the material will advance applications in biomedical devices, soft robotics, and flexible electronics. The versatile polymerization method shown here allows for facile changes of the filler composition to impart desired functionalities. Compared to current filled rubbers, the use and tailorability of polymer grafted nanoparticles allows for more ability to achieve differing dispersion states, which is an additional tuning knob to control material properties. Previous work has successfully shown the use of RIPT to disperse PGNPs in PS and PMMA systems due in part to matrix grafting on the particles as well as kinetic trapping in a glassy matrix. Here we adopted this method for the dispersion of PGNPs in PLMA, a rubbery matrix, to create soft hybrid elastomers. Utilizing a low crosslink density PLMA network with an elastic modulus of 104 kPa, nanoparticles were added in varied weight fractions spanning 1-10 wt% and were found to form PGNP clusters. The resulting mechanical properties show an increase in Young's modulus at low weight percentage and excellent recoverability when compared to a neat elastomer. Furthermore, additional work is needed to quantify the impact of crosslink density on particle dispersion. The low levels of crosslink density were hypothesized to optimize the measured influence of particle loading on modulus but may have mitigated the extent of particle trapping within the matrix. PGNPs are exciting materials, and the use of RIPT to synthesize hybrid materials will help expand the possibilities for functional soft hybrid elastomers.

4. Experimental Methods

4.1 Materials

Tetraethylorthosilicate (TEOS), ammonium hydroxide (28% in water), Grubbs' second-generation catalyst (G2), pentane, 3-bromopyridine (3BP), norbornene (NBE), ethyl vinyl ether,

lauryl methacrylate (LMA), benzoyl peroxide (BPO), hydrofluoric acid (49% aq.), 1,6-hexanediol dimethacrylate, and alumina were purchased from Sigma Aldrich. Ethanol (EtOH), tetrahydrofuran (THF), acetone, and isopropyl alcohol (IPA) were purchased from ThermoFisher Scientific. The silane, (5-bicyclo[2.2.1]hept-2-enyl)triethoxysilane (NBES), was purchased from Gelest. Microscopy grids purchased from ElectronMicroscopy Sciences were Formvar/Carbon 200 mesh with copper backing. All materials were used as received unless specified otherwise.

4.2 Methods

4.2.1 Silica Nanoparticle Synthesis and Surface Functionalization

Silica nanoparticles (NPs) are synthesized via a previously established Stöber process, resulting in spherical nanoparticles averaging 150-160 nm in diameter.[37] The NPs were produced by mixing 400 mL ethanol (EtOH), 26 mL of ammonium hydroxide (28% in water), and 12 mL tetraethylorthosilicate (TEOS) overnight. The NP surfaces are functionalized with norbornenyltriethoxylsilane (NBES) by adding an additional 400 mL of EtOH and 2 mL NBES and refluxing at 70 °C overnight, then distilling the solution at 110 °C the following day. Finally, the nanoparticles are purified via centrifugation (10,000 rpm, 20 min) and redispersion in tetrahydrofuran (THF), repeated three times, and stored in suspension in anhydrous THF at 3 °C.[34]

4.2.2 Grubbs' 3rd Generation Catalyst

Grubbs' 2nd generation catalyst (G2) was reacted with 10 molar excess of 3-bromopyridine (3BP) for 10 min, then the product is precipitated in 10 mL of pentane, filtered, vacuum dried, and stored in inert conditions.[47]

4.2.3 Surface-Initiated Ring-Opening Metathesis Polymerization (SI-ROMP) of Poly(norbornene) (PNBE)-Grafted Nanoparticles

SI-ROMP of PNBE was executed by following modified synthetic procedures obtained from previously published studies.[36] Under inert atmosphere, G3 (85 mg) is dissolved in anhydrous THF (2-3 mL) then silica nanoparticles (1.5 g in THF) are added. The particles stir in the catalyst solution for 15 min then 3BP (5 mL, 0.02 M in THF) is added and stirred for an additional min. To remove excess G3, the activated nanoparticle (ANP) solution is centrifuged (11,000 rpm, 7 min) in a sealed tube then sonicated and vortexed in fresh THF (anhydrous, 0.02 M 3BP) three times. A light centrifugation (2,500 rpm, 3 min) separates out large aggregates and the ANP supernatant is prepared for addition to the reaction vials.[34] Once the unreacted G3 is removed, the activated particles (~1 g) were added to NBE (38 g) in anhydrous THF (4M) with 3BP (0.02M). The polymerization was run for 5 s at ambient temperatures, then ethyl vinyl ether (5 mL) was injected to terminate the reaction (15 min). The PGNPs are purified via centrifugation (10,000 rpm, 20 min) then redispersed and stored in THF at 3 °C.[34]

4.2.4 Free Radical Polymerization of Poly(lauryl methacrylate) (PLMA) Elastomers

PLMA networks without nanoparticles were synthesized with varying degrees of crosslinking by combining LMA (7 mL), BPO (150 mg), and 1,6-hexanediol dimethacrylate (0.25-1.5 mol%). The LMA monomer was purified through a column of alumina before use. The mass of crosslinker was accurately obtained by utilizing a stock solution in acetone (16 mg/ml). The stock solution was transferred to vials and the acetone was evaporated off before adding the LMA and BPO.

Hybrid PLMA networks were synthesized with 0.25 mol% crosslinker and varied amounts of nanoparticle. The process above was used to add 1,6-hexanediol dimethacrylate (0.25 mol%) and BPO (150 mg) into a vial. PNBE grafted NPs were prepared by solvent switched from THF to LMA monomer by three cycles of centrifugation (10,000 rpm, 20 min) and redispersion in LMA. Next, the PGNP in LMA solutions were diluted with excess LMA (1-10 wt%) and 7 mL was added to the vials. Mixtures were sonicated until dissolved, distributed into square Teflon molds, and polymerized at 80 °C for 6 h. The products were then cooled, removed from the molds, and submerged in IPA overnight to swell and remove unreacted monomer. After swelling, the polymer networks were removed from the IPA and dried under vacuum at 50 °C (97% conversion).

4.2.5 Dynamic Light Scattering (DLS)

Dynamic light scattering (DLS) measurements are done using a Brookhaven Instruments BI-200SM Research goniometer system with a 637 nm, 30 mW laser, and a 100 μm aperture. The intensity autocorrelation function was recorded at room temperature using 4 detector angles (45°, 60°, 90°, 120°). Four separate measurements were taken at each angle and the average was used in analysis of the data. The autocorrelation function was analyzed using the CONTIN algorithm to determine the average diffusion coefficient, and the hydrodynamic diameter of the diffusing particles was calculated using the Stokes−Einstein relation. Samples are prepared in LMA (3 mg/ml) and filtered through 1 μm PTFE prior to characterization.

4.2.6 Polymer Cleavage via Hydrofluoric Acid and Size-Exclusion Chromatography with Multi-Angle Light Scattering Detector (SEC-MALS)

Polymer-grafted nanoparticles (100–250 mg in THF) are dissolved in 20 mL of THF before being added to a PTFE dish. 10 drops (~1 mL) of HF (49% aq.) are added to the dish and allowed to evaporate for 12 h under slow stirring.[48] Once the HF has evaporated, cleaved polymer samples (3–5 mg/mL THF) are prepared and filtered with 0.45 μm PTFE filter prior to characterization. SEC measurements are conducted in THF at 40 °C on a Tosoh EcoSEC equipped with a Wyatt Dawn Heleos-II eight angle light scattering detector.

4.2.7 Transmission Electron Microscopy (TEM)

Micrographs are taken with a FEI Tecnai G2 Spirit BioTwin transmission electron microscopy (TEM). Silica nanoparticle samples are prepared by drop casting 1 mg/mL THF solutions on to TEM grids. PGNP samples are prepared by placing TEM grids in a vial then adding 300 μL of 2-3 mg/ml THF solutions and allowing solvent evaporation overnight.[49] Dried hybrid elastomers were microtomed into 70–90 nm thin sheets using a Leica UC6 ultramicrotome.

4.2.8 Tensile Measurements

A metal punch was used to cut dog bone samples from the bulk elastomers prior to testing. Uniaxial extension tests were conducted using an MTS Exceed load frame with a 20 N transducer and 5 mm/min strain rate. After the samples were mounted, calipers were used to measure gauge length between grips while the width and thickness of the samples were measured at the center of the dog bone. Standard tests extended the samples until break. The Young's modulus (E) and tensile strength (TS) were determined from stress versus strain plots generated using the tensile data collected, each sample was run in triplicate and reported values are averages. Recovery tests extended the samples up to 50% strain in increments of 5%, for a total of 10 cycles, returning to

the initial position between each extension. For each sample with different nanoparticle compositions, 3 – 7 dog bone samples were prepared and measured.

ASSOCIATED CONTENT

Supporting Information

Supporting information can be found at doi…

AUTHOR INFORMATION

Corresponding Author

Email: rjh64@psu.edu

ORCID

Robert J. Hickey: 0000-0001-6808-7411

Jensen Sevening: 0000-0002-1934-0617

Siyana Dottin: 0000-0001-5504-1586

Vincent Torres: 0000-0003-0171-0664

Declaration of Competing Interests

We declare there are no conflicts or competing financial interest.

Acknowledgments

This work is supported by the National Science Foundation (NSF), Division of Materials Research Polymers Program (CAREER Proposal No.: DMR-1942508). TEM measurements were taken at

the Materials Characterization Lab (MCL) in the Materials Research Institute (MRI) at Penn State University. We thank Missy Hazen from the Huck Institute of the Life Science at Penn State for her help with TEM sample preparation.

References

(1) Li, Q.; Chen, L.; Gadinski, M. R.; Zhang, S.; Zhang, G.; Li, H.; Haque, A.; Chen, L.-Q.; Jackson, T.; Wang, Q. Flexible high-temperature dielectric materials from polymer nanocomposites. *Nature* **2015**, *523*, 576-579.

(2) Kim, P.; Doss, N. M.; Tillotson, J. P.; Hotchkiss, P. J.; Pan, M.-J.; Marder, S. R.; Li, J.; Calame, J. P.; Perry, J. W. High Energy Density Nanocomposites Based on Surface-Modified BaTiO3 and a Ferroelectric Polymer. *ACS Nano* **2009**, *3*, 2581-2592.

(3) Lebeau, B.; Innocenzi, P. Hybrid materials for optics and photonics. *Chem. Soc. Rev.* **2011**, *40*, 886-906.

(4) Kojima, Y.; Usuki, A.; Kawasumi, M.; Okada, A.; Fukushima, Y.; Kurauchi, T.; Kamigaito, O. Mechanical properties of nylon 6-clay hybrid. *J. Mater. Res.* **2011**, *8*, 1185-1189.

(5) Heinrich, G.; Klüppel, M.; Vilgis, T. A. Reinforcement of elastomers. *Curr. Opin. Solid State Mater. Sci.* **2002**, *6*, 195-203.

(6) Tsagaropoulos, G.; Eisenberg, A. Dynamic Mechanical Study of the Factors Affecting the Two Glass Transition Behavior of Filled Polymers. Similarities and Differences with Random Ionomers. *Macromolecules* **1995**, *28*, 6067-6077.

(7) Wu, D.; Ge, Y.; Li, R.; Feng, Y.; Akcora, P. Thermally Activated Shear Stiffening in Polymer-Grafted Nanoparticle Composites for High-Temperature Adhesives. *ACS Appl. Polym. Mater.* **2022**, *4*, 2819-2827.

(8) Kumar, S. K.; Jouault, N.; Benicewicz, B.; Neely, T. Nanocomposites with Polymer Grafted Nanoparticles. *Macromolecules* **2013**, *46*, 3199-3214.

(9) Akcora, P.; Liu, H.; Kumar, S. K.; Moll, J.; Li, Y.; Benicewicz, B. C.; Schadler, L. S.; Acehan, D.; Panagiotopoulos, A. Z.; Pryamitsyn, V.; Ganesan, V.; Ilavsky, J.; Thiyagarajan, P.; Colby, R. H.; Douglas, J. F. Anisotropic self-assembly of spherical polymer-grafted nanoparticles. *Nat. Mater.* **2009**, *8*, 354-359.

(10) Mackay, M. E.; Tuteja, A.; Duxbury, P. M.; Hawker, C. J.; Van Horn, B.; Guan, Z.; Chen, G.; Krishnan, R. S. General Strategies for Nanoparticle Dispersion. *Science* **2006**, *311*, 1740-1743.

(11) Kumar, S. K.; Benicewicz, B. C.; Vaia, R. A.; Winey, K. I. 50th Anniversary Perspective: Are Polymer Nanocomposites Practical for Applications? *Macromolecules* **2017**, *50*, 714-731.

(12) Zoppe, J. O.; Ataman, N. C.; Mocny, P.; Wang, J.; Moraes, J.; Klok, H.-A. Surface-Initiated Controlled Radical Polymerization: State-of-the-Art, Opportunities, and Challenges in Surface and Interface Engineering with Polymer Brushes. *Chem. Rev.* **2017**, *117*, 1105-1318.

(13) Choi, C.; Okayama, Y.; Morris, P. T.; Robinson, L. L.; Gerst, M.; Speros, J. C.; Hawker, C. J.; Read de Alaniz, J.; Bates, C. M. Digital Light Processing of Dynamic Bottlebrush Materials. *Adv. Funct. Mater.* **2022**, *32*, 2200883.

(14) Xie, R.; Mukherjee, S.; Levi, A. E.; Reynolds, V. G.; Wang, H.; Chabinyc, M. L.; Bates, C. M. Room temperature 3D printing of super-soft and solvent-free elastomers. *Sci. Adv.*, *6*, eabc6900.

(15) Kim, S.; Laschi, C.; Trimmer, B. Soft robotics: a bioinspired evolution in robotics. *Trends Biotechnol.* **2013**, *31*, 287-294.

(16) Vatankhah-Varnoosfaderani, M.; Daniel, W. F. M.; Zhushma, A. P.; Li, Q.; Morgan, B. J.; Matyjaszewski, K.; Armstrong, D. P.; Spontak, R. J.; Dobrynin, A. V.; Sheiko, S. S. Bottlebrush Elastomers: A New Platform for Freestanding Electroactuation. *Adv. Mater.* **2017**, *29*, 1604209.

(17) Pelrine, R.; Kornbluh, R.; Pei, Q.; Joseph, J. High-Speed Electrically Actuated Elastomers with Strain Greater Than 100%. *Science* **2000**, *287*, 836-839.

(18) Madsen, F. B.; Daugaard, A. E.; Hvilsted, S.; Skov, A. L. The Current State of Silicone-Based Dielectric Elastomer Transducers. *Macromol. Rapid Commun.* **2016**, *37*, 378-413.

(19) Seifert, J.; Günzing, D.; Webers, S.; Dulle, M.; Kruteva, M.; Landers, J.; Wende, H.; Schmidt, A. M. Strain- and field-induced anisotropy in hybrid elastomers with elongated filler nanoparticles. *Soft Matter* **2021**, *17*, 7565-7584.

(20) Seifert, J.; Roitsch, S.; Schmidt, A. M. Covalent Hybrid Elastomers Based on Anisotropic Magnetic Nanoparticles and Elastic Polymers. *ACS Appl. Polym. Mater.* **2021**, *3*, 1324-1337.

(21) Borin, D.; Stepanov, G.; Dohmen, E. Hybrid magnetoactive elastomer with a soft matrix and mixed powder. *Arch. Appl. Mech.* **2019**, *89*, 105-117.

(22) Karimkhani, V.; Vatankhah-Varnosfaderani, M.; Keith, A. N.; Dashtimoghadam, E.; Morgan, B. J.; Jacobs, M.; Dobrynin, A. V.; Sheiko, S. S. Tissue-Mimetic Dielectric Actuators: Free-Standing, Stable, and Solvent-Free. *ACS Appl. Polym. Mater.* **2020**, *2*, 1741-1745.

(23) Li, Y.; Thouas, G. A.; Chen, Q.-Z. Biodegradable soft elastomers: synthesis/properties of materials and fabrication of scaffolds. *RSC Advances* **2012**, *2*, 8229-8242.

(24) Cai, M.; Nie, S.; Du, Y.; Wang, C.; Song, J. Soft Elastomers with Programmable Stiffness as Strain-Isolating Substrates for Stretchable Electronics. *ACS Appl. Mater. Interfaces* **2019**, *11*, 14340-14346.

(25) Akcora, P.; Kumar, S. K.; Moll, J.; Lewis, S.; Schadler, L. S.; Li, Y.; Benicewicz, B. C.; Sandy, A.; Narayanan, S.; Ilavsky, J.; Thiyagarajan, P.; Colby, R. H.; Douglas, J. F. "Gel-like" Mechanical Reinforcement in Polymer Nanocomposite Melts. *Macromolecules* **2010**, *43*, 1003-1010.

(26) Bouty, A.; Petitjean, L.; Chatard, J.; Matmour, R.; Degrandcourt, C.; Schweins, R.; Meneau, F.; Kwasńiewski, P.; Boué, F.; Couty, M.; Jestin, J. Interplay between polymer chain conformation and nanoparticle assembly in model industrial silica/rubber nanocomposites. *Faraday Discuss.* **2016**, *186*, 325-343.

(27) Baeza, G. P.; Genix, A.-C.; Paupy-Peyronnet, N.; Degrandcourt, C.; Couty, M.; Oberdisse, J. Revealing nanocomposite filler structures by swelling and small-angle X-ray scattering. *Faraday Discuss.* **2016**, *186*, 295-309.

(28) LaNasa, J. A.; Neuman, A.; Riggleman, R. A.; Hickey, R. J. Investigating Nanoparticle Organization in Polymer Matrices during Reaction-Induced Phase Transitions and Material Processing. *ACS Appl. Mater. Interfaces* **2021**, *13*, 42104-42113.

(29) LaNasa, J. A.; Torres, V. M.; Hickey, R. J. In situ polymerization and polymer grafting to stabilize polymer-functionalized nanoparticles in polymer matrices. *J. Appl. Phys.* **2020**, *127*, 134701.

(30) Fischer, M.; Hellmann, G. P. On the Evolution of Phase Patterns during the High-Impact-Modified Polystyrene Process. *Macromolecules* **1996**, *29*, 2498-2509.

(31) Torres, V. M.; LaNasa, J. A.; Vogt, B. D.; Hickey, R. J. Controlling nanostructure and mechanical properties in triblock copolymer/monomer blends via reaction-induced phase transitions. *Soft Matter* **2021**, *17*, 1505-1512.

(32) Zofchak, E. S.; LaNasa, J. A.; Mei, W.; Hickey, R. J. Polymerization-Induced Nanostructural Transitions Driven by In Situ Polymer Grafting. *ACS Macro Lett.* **2018**, 822-827.

(33) Zofchak, E. S.; LaNasa, J. A.; Torres, V. M.; Hickey, R. J. Deciphering the Complex Phase Behavior during Polymerization-Induced Nanostructural Transitions of a Block Polymer/Monomer Blend. *Macromolecules* **2020**, *53*, 835-843.

(34) LaNasa, J. A.; Hickey, R. J. Surface-Initiated Ring-Opening Metathesis Polymerization: A Method for Synthesizing Polymer-Functionalized Nanoparticles Exhibiting Semicrystalline Properties and Diverse Macromolecular Architectures. *Macromolecules* **2020**, *53*, 8216-8232.

(35) Pribyl, J.; Benicewicz, B.; Bell, M.; Wagener, K.; Ning, X.; Schadler, L.; Jimenez, A.; Kumar, S. Polyethylene Grafted Silica Nanoparticles Prepared via Surface-Initiated ROMP. *ACS Macro Lett.* **2019**, *8*, 228-232.

(36) Jordi, M. A.; Seery, T. A. P. Quantitative Determination of the Chemical Composition of Silica−Poly(norbornene) Nanocomposites. *J. Am. Chem. Soc.* **2005**, *127*, 4416-4422.

(37) Ohno, K.; Morinaga, T.; Koh, K.; Tsujii, Y.; Fukuda, T. Synthesis of Monodisperse Silica Particles Coated with Well-Defined, High-Density Polymer Brushes by Surface-Initiated Atom Transfer Radical Polymerization. *Macromolecules* **2005**, *38*, 2137-2142.

(38) Bielawski, C. W.; Grubbs, R. H. Living ring-opening metathesis polymerization. *Prog. Polym. Sci.* **2007**, *32*, 1-29.

(39) Louie, J.; Grubbs, R. H. Metathesis of Electron-Rich Olefins: Structure and Reactivity of Electron-Rich Carbene Complexes. *Organometallics* **2002**, *21*, 2153-2164.

(40) Moh, L. C. H.; Losego, M. D.; Braun, P. V. Solvent Quality Effects on Scaling Behavior of Poly(methyl methacrylate) Brushes in the Moderate- and High-Density Regimes. *Langmuir* **2011**, *27*, 3698-3702.

(41) Ethier, J. G.; Hall, L. M. Structure and Entanglement Network of Model Polymer-Grafted Nanoparticle Monolayers. *Macromolecules* **2018**, *51*, 9878-9889.

(42) Ethier, J. G.; Hall, L. M. Modeling individual and pairs of adsorbed polymer-grafted nanoparticles: structure and entanglements. *Soft Matter* **2018**, *14*, 643-652.

(43) He, D.; Jiang, B. The elastic modulus of filled polymer composites. *J. Appl. Polym. Sci.* **1993**, *49*, 617-621.

(44) Hou, D.; Bostwick, J. E.; Shallenberger, J. R.; Zofchak, E. S.; Colby, R. H.; Liu, Q.; Hickey, R. J. Simultaneous Reduction and Polymerization of Graphene Oxide/Styrene Mixtures To Create Polymer Nanocomposites with Tunable Dielectric Constants. *ACS Appl. Nano Mater.* **2020**, *3*, 962-968.

(45) Moll, J. F.; Akcora, P.; Rungta, A.; Gong, S.; Colby, R. H.; Benicewicz, B. C.; Kumar, S. K. Mechanical Reinforcement in Polymer Melts Filled with Polymer Grafted Nanoparticles. *Macromolecules* **2011**, *44*, 7473-7477.

(46) Maillard, D.; Kumar, S. K.; Fragneaud, B.; Kysar, J. W.; Rungta, A.; Benicewicz, B. C.; Deng, H.; Brinson, L. C.; Douglas, J. F. Mechanical Properties of Thin Glassy Polymer Films Filled with Spherical Polymer-Grafted Nanoparticles. *Nano Lett.* **2012**, *12*, 3909-3914.

(47) Love, J. A.; Morgan, J. P.; Trnka, T. M.; Grubbs, R. H. A Practical and Highly Active Ruthenium-Based Catalyst that Effects the Cross Metathesis of Acrylonitrile. *Angew. Chem. Int. Ed.* **2002**, *41*, 4035-4037.

(48) Chancellor, A. J.; Seymour, B. T.; Zhao, B. Characterizing Polymer-Grafted Nanoparticles: From Basic Defining Parameters to Behavior in Solvents and Self-Assembled Structures. *Anal. Chem.* **2019**, *91*, 6391-6402.

(49) Bodnarchuk, M. I.; Kovalenko, M. V.; Heiss, W.; Talapin, D. V. Energetic and Entropic Contributions to Self-Assembly of Binary Nanocrystal Superlattices: Temperature as the Structure-Directing Factor. *J. Am. Chem. Soc.* **2010**, *132*, 11967-11977.